

Effects of E-Beam Irradiation on the Chemical, Thermal, and Mechanical Properties of Polyamide-6, Polyamide-6.6, and Polypropylene Used in Conveyor Belt Rollers

Juliana Arquinto^{a*} , Julio Harada^a , Dione Pereira de Castro^a ,
Leonardo Gondim de Andrade e Silva^a 

^aComissão Nacional de Energia Nuclear (CNEN), Instituto de Pesquisas Energéticas e Nucleares (IPEN), São Paulo, SP, Brasil.

Received: January 09, 2025; Revised: July 23, 2025; Accepted: August 03, 2025

In this study, polyamide 6 (PA 6), polyamide 6.6 (PA 6.6), and polypropylene (PP) polymers were irradiated with an e-beam (EB) (100 and 200 kGy doses, 100 kGy.s⁻¹ dose rate, at room temperature) to evaluate the effects on radiochemical crosslinking. Mechanical analyses (tensile, flexural, and tribological tests), thermal characterizations (TGA, DSC, and glow wire test), and FTIR spectroscopy were performed. Results demonstrated that PA 6.6 irradiated at 200 kGy exhibited a 6.8% increase in tensile strength at break, being the only material showing improvement in yield point. All samples displayed reduced elongation after irradiation. In flexural resistance tests, both irradiated PA 6 and PA 6.6 showed enhanced properties, while in tribological evaluations, only PA 6.6 (100 kGy) presented a reduced friction coefficient. Thermal analyses revealed that irradiated PA 6.6 showed increased onset degradation temperature, while all polymers exhibited decreased melting temperature. The crystallinity percentage increased in both irradiated PA 6.6 and PP, and only PA 6.6 (200 kGy) resisted all temperature levels in the glow wire test. It was concluded that PA 6.6 demonstrated superior post-irradiation performance, showing more enhanced properties compared to PA 6 and PP.

Keywords: Polyamide-6, polyamide-6.6, polypropylene, electron beam irradiation, irradiation processing.

1. Introduction

The physical and chemical alterations in polymer's properties caused by energy transfer from incidental ionizing radiation are primarily driven by the competition between crosslinking and chain scission processes^{1,2}. These phenomena are largely influenced by polymer structure, irradiation atmosphere, and exposure temperature. Injection-molded polymers typically undergo radiation-induced crosslinking through the recombination of free radicals generated during electron beam treatment using electron accelerators³. The effects of high-energy radiation transferred by accelerated electrons on polyamides^{1,2,4-6} and polypropylene⁷⁻⁹ have been extensively investigated by various researchers.

Among the characteristics of PA-6 and PA-6.6 is their high-water absorption, which becomes more pronounced at higher ambient humidity levels². Absorbed water acts as a plasticizing effect, especially in PA-6 and PA-6.6. While also reducing the material's tensile strength and modulus¹⁰. Furthermore, polyamides have high thermal stability, but this can be compromised when the absorption of thermal, light, or mechanical energy^{4,5,10}. The degree of chain scission and crosslinking reactions primarily depends on the energy loss mechanism and the material's stability when these products are exposed to high-energy radiation^{11,12}.

The water absorption and crystallization behavior of polyamides depends on moisture exposure duration, since prolonged contact with humidity induces random structural changes in the polymer backbone. Pramanik et al.² evaluate the behavior of the Nylon[®] 6 when it is treated by EB irradiation in air at ambient temperature, reaching superior improved performances in comparison with those shown by unirradiated samples. For instance, Bradler et al.¹³ investigated the effects of five different irradiation doses in the range of 0 - 200 kGy. Accordingly, various crosslinked PA grades were obtained. Adem et al.⁴ studied the effects of EB irradiation on the ameliorated mechanical properties of PA-6 and PA-6.6. The selected irradiation doses⁴ produce an increase in the tensile strength as the dose is enhanced, while these processing conditions limit the narrower value range of properties. However, it allows us to establish a correlation between the scratch hardness and the effective contact pressure developed between the indenter and the scratched surface. The studied polymer mechanical properties became convenient for several applications¹⁴⁻¹⁸. Svoboda et al.⁸ studied a linear PP modified employing EB treatment with irradiation dose increase. The formation of new molecular branches along the main chain was observed. However, as the dose became higher, the structuration process continued to produce several shorter branches per molecule, modifying the chemical structure of the resin. Finally, it is also observed that PP exhibits a high degradation rate when it is exposed to

*e-mail: juliana_arquinto@hotmail.com

Associate Editor: Walney Araújo.

Editor-in-Chief: Luiz Antonio Pessan.

ionizing radiation, even at low doses, leading to significantly reduced resistance against aging, weathering, and irradiation⁹.

Sirin et al.¹⁹ observed that crosslinking rather than oxidative degradation occurs in polypropylene and polyethylene blends at high EB doses. In addition, during the irradiation of polyamides in the presence of oxygen, a typical radical scavenger, the oxidation of the material leads to the ageing of the polymer by the decay of free radicals^{6,9,12}. Only a few works reported changes induced by irradiation on injection-molded specimens^{3,10,12}. In this study, PA-6, PA-6.6, and PP were treated with EB to enhance their performance for further use in industrial conveyor belt rollers. The EB treatment is expected to create crosslinked structures in the samples studied, contributing to the improved physical and mechanical properties of the irradiated materials.

2. Experimental

2.1. Materials

PA-6, PA-6.6 (Sollamid B, Krissoll®), and PP (PP Standard grade, Braskem®) were provided by manufacturing companies. The test samples were obtained by injection molding. The samples were prepared according to ASTM D638 and D790. PA-6 and PA-6.6 samples are characterized by their tendency to absorb water. For this goal, a drying step is necessary before injection molding and irradiation processes. After the injection, the samples were hydrated.

2.2. Sample preparation

The hydration parameters of the samples of PA-6 and PA-6.6 were calculated as the average of 10 specimens performed after injection molding following the literature were as follows²⁰: water temperature 70–80°C and time of 2 hours. This information can be found in Table 1.

2.3. Irradiation method

The prepared samples were irradiated with an electron beam accelerator, Dynamitron® DC1500/25 (JOB 188 model) with a maximal energy output of 1.5 MeV, at a dose rate of 100 kGy.s⁻¹. The irradiation doses were set between 100 and 200 kGy under ambient air conditions. The samples were positioned on a custom-designed support developed by the Radiation Technology Center at IPEN/CNEN.

2.4. Characterization

The Fourier-transform infrared spectroscopy (FTIR-ATR) spectra were recorded in a Perkin-Elmer Spectrum™ 3 model with 32 scans. The tensile strength tests were conducted according to the parameters specified in the ASTM D638 standard, with adaptations for a 10 N load cell and a speed of 50 mm·min⁻¹. The flexural tests were accomplished as it is specified in the ASTM D790. Both these mechanical

tests were performed in an Instron® 5567 equipment located at the Radiation Technology Center, IPEN/CNEN. The thermal properties and the variation of melting point (T_m) and enthalpy (ΔH) were studied on the absorbed dose range in a nitrogen atmosphere, at temperatures between 20 and 600°C at a heating rate of 20°C min⁻¹. Simultaneously, TGA-DSC equipment was used (Mettler Toledo® 3). A glow wire test was used to determine the thermal resistance in the samples, irradiated and non-irradiated. This characterization allows the identification of the physical-chemical changes and the behavior of samples at three temperatures (650, 750, and 850°C). Scratch testing was conducted on a Bruker® DFH-10 tribometer under ASTM G171 standard using a 5 N load, 0.2–5 mm/s speed, and 4 mm scratch length. Tests were performed with a cylindrical indenter at 90° to the sample surface. The microstructural surface analysis after scratch tests was collected using a Taylor Robson® CCI 3D-profilometer, for different magnifications. All these data were analyzed statistically using ANOVA tests. When the null hypothesis was rejected, Tukey's tests ($p < 0.05$) were applied for mean comparisons.

3. Results and Discussion

3.1. Fourier-transform infrared spectroscopy

The FTIR spectra of the raw materials and samples are presented in Figures 1a-c. FTIR analysis reveals that the spectral characteristics of PA-6 remained unchanged when the samples were irradiated with doses between 100 and 200 kGy indicating a significant chemical stability. This behavior may be learned because the fundamental chemical groups were not affected. The distinctive characteristics of PA-6 are manifested by secondary amide groups, evidenced by a -NH stretching band around 3300 cm⁻¹, C-H group stretching vibrations in the 3000 ± 150 cm⁻¹ range, the presence of the C=O group in the 1680 to 1630 cm⁻¹ region, and the (CH₂)_n vibrations between 1500 and 900 cm⁻¹ in the spectra^{21,22}. The band ascribed to carbonyl (-C=O) groups appears broader with the increase in the irradiation dose applied²³. Zaharescu et al.¹¹ investigated the dependence of absorbance on the pre-irradiation dose and heating time for the 1652 cm⁻¹ specifically observed during the thermal degradation of PA-6 and PA-6.6 specimens γ -treated at 100 kGy. Porubská et al.¹² described the accumulation of these amine groups in EB radiated PA-6 samples. The modifications foreseen appeared to be insignificant when compared to virgin PA-6 indicating that such changes do not likely to occur.

The discussion on the radiation effects brought about by EB shows that the spectral characteristics of PA-6.6 remain unchanged when subjected to radiation with doses of 100 and 200 kGy, as shown previously, indicating preservation of its essential chemical groups in the structure of PA-6.6. The characteristic bands of PA-6.6 show marked similarities to those of PA-6. PA degradation is commonly also indicated by hydroxyl groups (-OH), as shown by 3500 cm⁻¹ and carbonyl groups (1736 cm⁻¹), but there was no trace of these groups modified in this spectral area^{1,6}. The secondary amide groups are identified by a band (-NH) around 3300 cm⁻¹. Any absorption in the 3000 ± 150 cm⁻¹ range is predominantly

Table 1. PA-6 and PA-6.6 hydration process final average.

Specimen	M_0 (g)	M_f (g)	Hydration final (%)
PA-6	10.1847	10.5682	3.77%
PA-6.6	9.8952	10.1458	2.53%

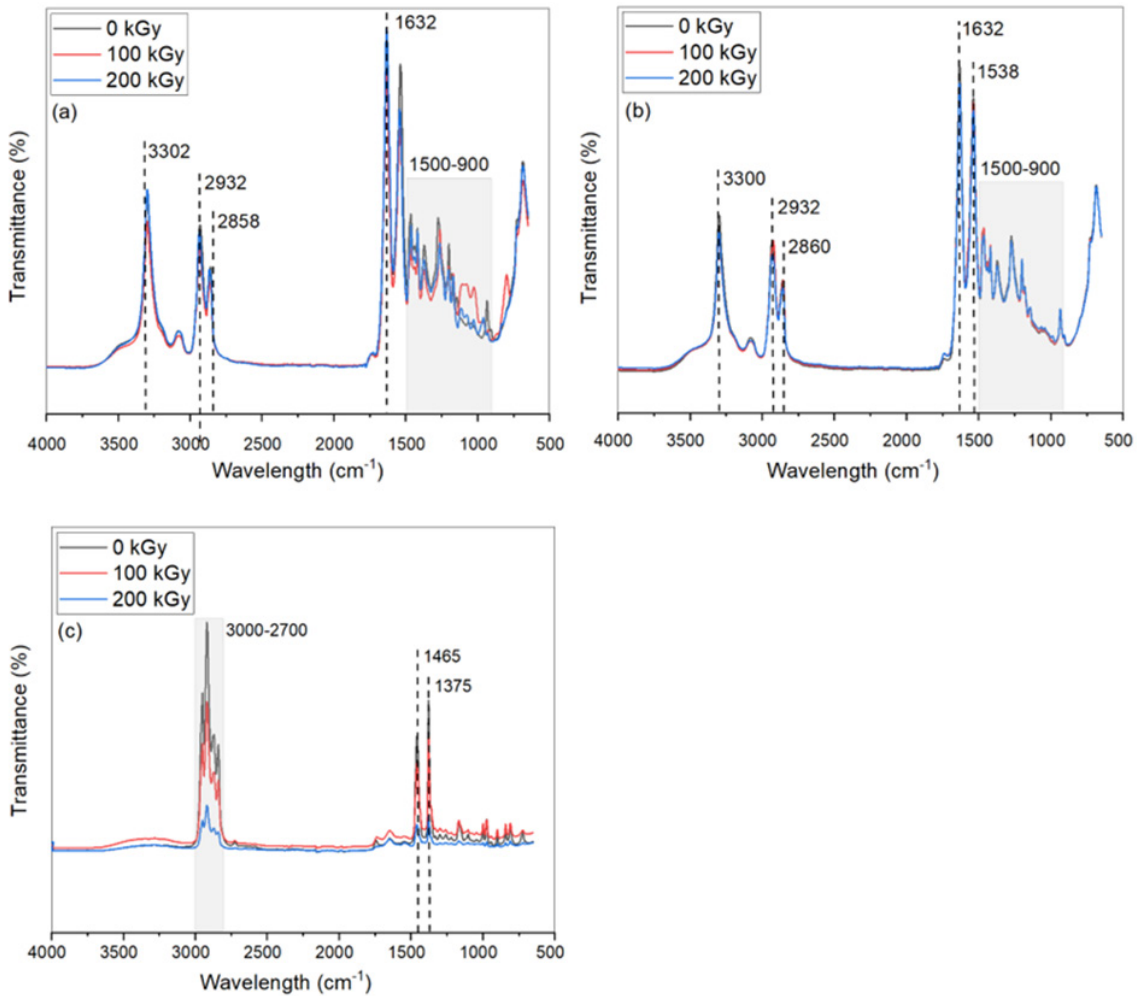


Figure 1. FTIR spectra for 0 kGy, 100 kGy, and 200 kGy samples of PA-6 (a), PA-6.6 (b), and PP (c).

attributed to the presence of the C-H bond, a typical stretching pattern. In the 1680 to 1630 cm⁻¹ region, there is an intense absorption band for the C=O group. In a series of aliphatic polyamides, where the number of methylene groups is increased, differences in the vibrational spectra in the 1500-900 cm⁻¹ range can be identified³. These variations are mainly the result of bands associated with the bending and twisting vibrations of the CH₂ group in the C-C chain structure^{21,22}. Burillo et al.¹ describe that the irradiation process in the PA-polymer can be associated with radiolysis promoted by water in the PA-side groups to be observed by FTIR, where the predominant effects are main chain scission and crosslinking of the polymer. Polyamides have much structural similarity with linear polyethylene, and it is the presence of the -CONH- groups that causes polyamides to differ from polyolefin groups^{2,23}.

Scission chain has been reported in numerous studies on the irradiation of PA grades using accelerated electrons or gamma rays, where the cleavage mechanism (1) (Figure 2) proposes the formation of relatively unstable macroradicals, which are decomposed through a unimolecular process into alkoxy radicals^{1,24}.

From the characteristics of PP, it may be observed that the spectral absorption bands remain unaltered after being subjected to radiation. However, the bands were less intense, as can be seen in Figure 1c. This fact indicates that the material was degraded during its local scission, and the chain size in the range of 2700-3000 cm⁻¹⁸. The C-H stretching vibrations of the -CH-, -CH₂-, and -CH₃ groups are observed together with the CH₂ and CH₃ bending bands in the range of 1475 to 1365 cm⁻¹. As it was previously reported^{21,22} alkanes whose class includes polypropylene generally show few absorption bands in the infrared spectrum. Interestingly, any evident induction period is not observed during the free radical degradation^{24,25}.

In the spectra of PP samples, a new absorption band at the 1716 cm⁻¹ range appears, with its intensity increasing as the dose rises. These post-irradiation change is ascribed to the formation of carbonyl or hydroxyl groups they being the precursors of resulting aldehydes and ketones produced by the interaction of oxygen molecules with free radicals trapped in PP chains during the chain scission reaction^{9,25}. The PP cleavage mechanism (2) (Figure 3) proposes the

formation of relatively unstable macroradicals, as it was previously reported^{19,25}.

3.2. Mechanical properties

The mechanical properties of the samples are presented in Figures 4–6. The analysis of the tensile strength test on PA-6 suggests that there is a reduction in the corresponding values of tensile strength of 10.98 and 11.41% for the samples irradiated with doses of 100 and 200 kGy, respectively, with respect to non-irradiated samples. Table S1 (Supplementary material) shows the statistical data for the mechanical properties of PA-6.

For all PA specimens, the Young's modulus increased with irradiation doses up to 150 kGy. However, the further increases in the irradiation dose resulted in a decrease in Young's modulus according to the published results^{6,10,13}. Looking at the elongation results of the PA-6 samples, it may be remarked a significant reduction in this property may be observed when their references are compared to the non-irradiated samples. The reductions of 184.03 and 219.57% for the samples irradiated with doses of 100 and 200 kGy, respectively, may be noticed. Pramanik et al.² and Bradler et al.¹³ obtained similar results when a drop in elongation values occurred for similar irradiation. Figure 5 shows the effect of ionizing radiation on the mechanical

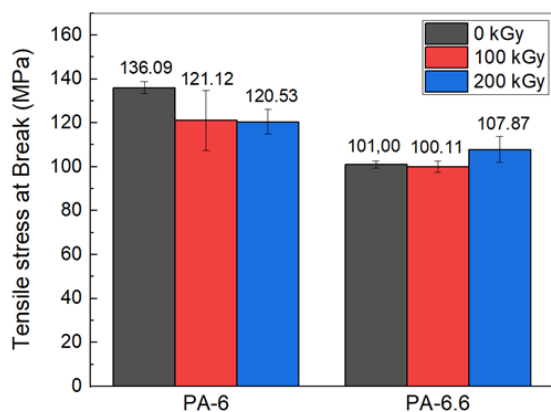


Figure 4. Tensile stress of non-irradiated and irradiated PA-6, and PA-6.6.

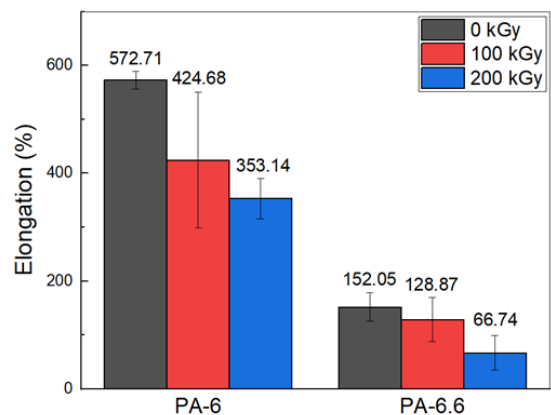


Figure 5. Elongation of non-irradiated and irradiated PA-6, and PA-6.6.

elongation properties of PA-6 grades. The analysis of yield point stress revealed reductions of 6.56 and 2.42% in PA-6's yielding capacity when irradiated at 100 and 200 kGy, respectively, compared to non-irradiated samples. Figure 6 shows the effect of ionizing radiation on the mechanical properties of tension at the yield point of PA-6.

In the tensile strength tests, PA-6.6 exposed to 100 kGy shows a reduction of 0.89% in comparison with the non-irradiated sample. However, when the dose becomes 200 kGy, the same material showed an increase of 6.8% compared to the non-irradiated sample. Table S2 shows the statistical data on the tensile mechanical properties of PA-6.6. The elongation results (Figure 5) of the PA-6.6 samples showed a decrease of 23 and 85.31%, when the irradiation-doses of 100 and 200 kGy, respectively. PA-6.6 showed an increase in its yield strength when subjected to radiation with doses of 100 and 200 kGy. Similar results were recorded by Pino and Colombo²⁶ and Sengupta et al.²⁷ in their earlier studies. Figure 6 shows the effect of ionizing radiation on the mechanical properties of tension at the yield point of PA-6.6.

After irradiation of the PP, an increase in the stiffness of the samples was observed. However, when they were adjusted to the tensile equipment, the samples broke at the clamping point, making it impossible to continue the testing. On the other hand, the higher EB doses may adversely cause the chain scission PA that brings about the deterioration of impact strength and tensile stress at break¹⁰. In the literature, it is reported that the irradiation of pure polypropylene samples can lead to β -scission occurring on the surface¹⁹.

Figure 7 shows the flexure stress of PA-6, PA-6.6, and PP samples with a limit of 5% mechanical deformation, and Table S3 shows the flexural statistical data. A slight increase in flexural tensile capacity of 7.3% can be seen when PA-6 was irradiated with a dose of 100 kGy, and an increase of 9.63% when the irradiation dose reached 200 kGy (Figure 7). Pramanik et al.² also observed that the flexural strength of PA-6 samples increased steadily as the irradiation dose increased. For the PA-6.6 sample, a slight increase in bending stress capacity of 1.62% is noticeable when the dose of 100 kGy was applied. Simultaneously, an increase of 8.29% was obtained when the dose was 200 kGy (Figure 7). When PA-6.6 is exposed to an EB dose of 200 kGy, Ferro²⁸ and Pramanik et al.¹⁰ observed a

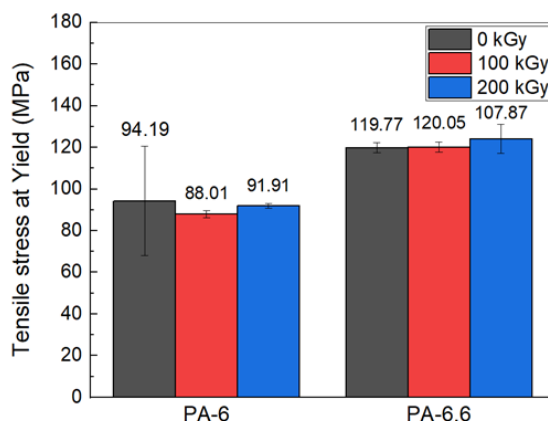


Figure 6. Tensile stress at yield of non-irradiated and irradiated PA-6, and PA-6.6.

similar behavior, when it was possible to notice an increase in flexural strength as a function of the increase in the enhanced dose transferred onto the polymer. On the other hand, the PP samples showed a slight decrease in bending stress capacity of approximately 10.21 and 9.9%, when irradiation doses were 100 and 200 kGy, respectively.

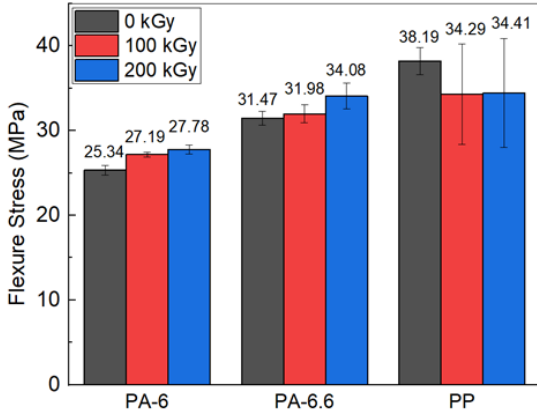


Figure 7. Flexure stress of non-irradiated and irradiated PA-6, PA-6.6, and PP.

3.3. Thermal properties

The non-irradiated PA-6 showed a higher degradation onset temperature compared to the irradiated samples, indicating that the degradation of the material began at lower temperatures for the irradiated samples. Figure 8 shows the TGA curves obtained from the PA-6 (a), PA-6.6 (b), and PP (c). Table S4 describes the statistical data used for the initial T_{onset} and final T_{endset} of the samples performed.

The TGA showed a slight weight decrease starting just above 100°C, attributed to the vaporization of the absorbed water, which can affect the thermal and mechanical properties of the material^{4,13}. The non-irradiated PA-6 (Figure 8a) presents a higher degradation temperature (T_{onset}) concerning the irradiated samples. It suggests that the degradation of the material began at lower temperatures for the irradiated samples. This effect is evidenced in Table S4 and Figure 8b, where polyamide irradiated with 100 kGy showed an increase of 1.19% in the T_{onset} value of degradation temperature relative to the non-processed sample. The irradiation of 200 kGy causes an increase of 5.34% over this same temperature range. PP and PA-6 samples showed a decrease in the T_{onset} of degradation after irradiation, as it was previously reported^{4,9}. Santos⁷ also identified a drop in the T_{onset} of degradation in PP samples (Figure 8c), after irradiation at 200 kGy. In this case, residual

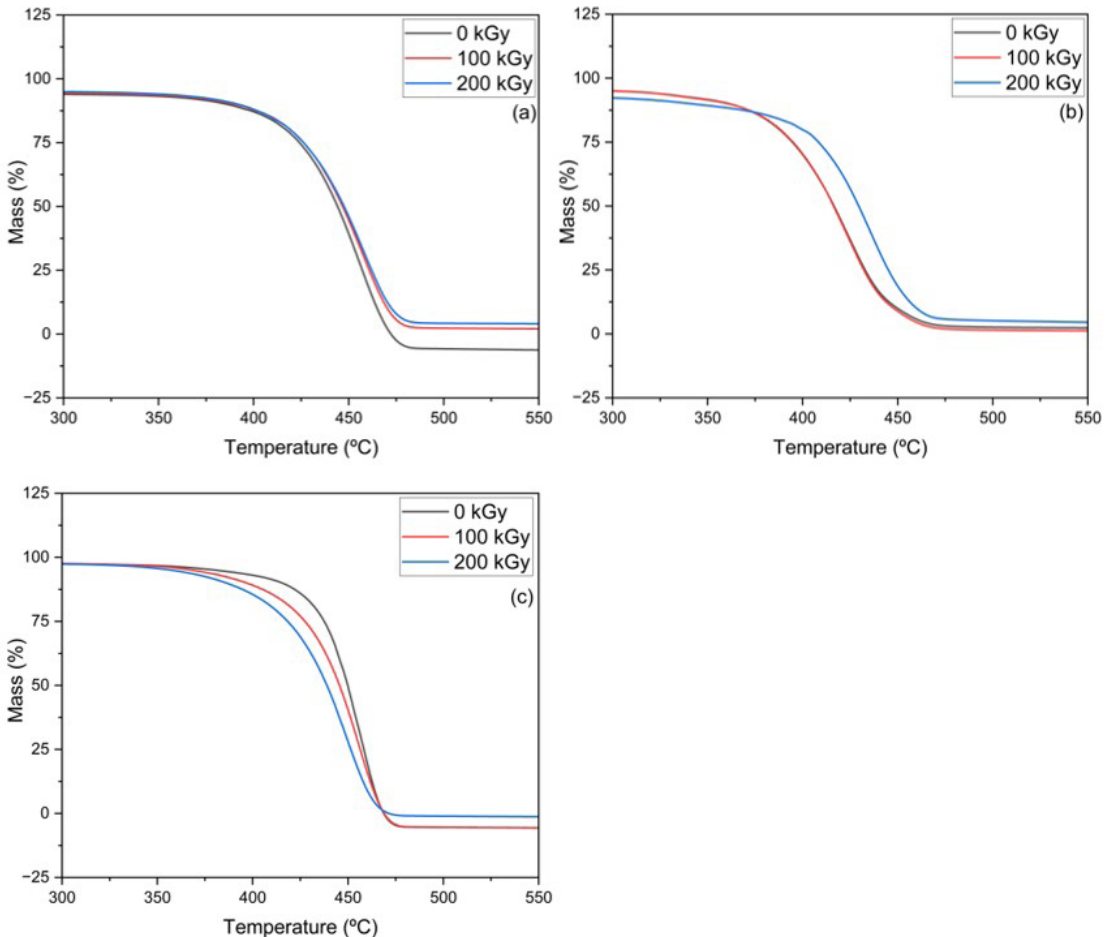


Figure 8. TGA curves of non-irradiated and irradiated PA-6 (a), PA-6.6 (b), and PP (c).

ashes from PA and PP increased with the irradiation dose⁴, although this change is small, as observed in the Figures 8a-c.

The heating curves obtained from the DSC analysis are shown in Figures 9a-c, both in the non-irradiated form and processed sample at 100 and 200 kGy. The corresponding values for melting temperature (T_m) and crystallization percentage data obtained are shown in Table S5. Figure 7a shows the heating curves for PA-6, where it can be seen that as the irradiation dose increases, there is a gradual decrease in the melting point and crystallinity index^{1,24}. This reduction can be attributed to a decrease¹³ in the crystalline structure of the irradiated samples, a similar phenomenon described by Park et al.²⁹ when the investigated samples of PA-6 at 100 and 200 kGy, by EB, alter the morphological structure. The decrease in the intensity of the crystalline absorption band by FTIR after irradiation suggests a significant reduction in the final crystallinity of the samples. Burillo et al.¹ studied the decreased melting point ($\sim 1\%$) for PA polymer samples with 1000 kGy at 50 and 70°C. Figure 9b shows the heating curves for PA-6.6, both non-irradiated and irradiated with doses of 100 and 200 kGy. After irradiation, PA-6.6 showed an increase in crystallinity of 1.41 and 2.2%, respectively, similar to the literature reference⁴. The melting temperature gradually decreased as the irradiation dose increased²⁴. This behavior is different

from the studies carried out by Park et al.²⁹, where both the crystallinity and melting temperature of PA-6.6 decreased when the polymer was subjected to radiation at 100 and 200 kGy. In both cases, the change in T_m was attributed to crosslinking and branching occurring primarily in the amorphous regions and at the boundaries of the crystallites^{4,24}. However, crosslinks are formed predominantly in the amorphous regions in the presence of the coagent or chemical modifiers²⁴.

For PP samples (Figure 9c) after irradiation, there was a slight increase⁹ in the crystallization percentage of PP of 1.41 and 1.45%, respectively, after exposure to doses of 100 and 200 kGy. Concerning the melting point, there was found a decrease in value of temperature value of 3.26 and 7.35%, respectively, was found after EB irradiation. Similar results were observed in the studies performed by Lugão et al.³⁰, Santos⁷, Sirin et al.¹⁹, and Svoboda et al.⁸ in which polypropylene irradiated at different doses showed a decrease in the melting temperature, including the crystallization kinetics motivated by the increased level of irradiation effects that caused a decrease in the number of nucleation centers in the PP polymer specimen.

3.4. Glow-wire test

All data concerning the glow-wire testing on the PA-6, PA-6.6, and PP samples are shown in Table 2. It can be seen

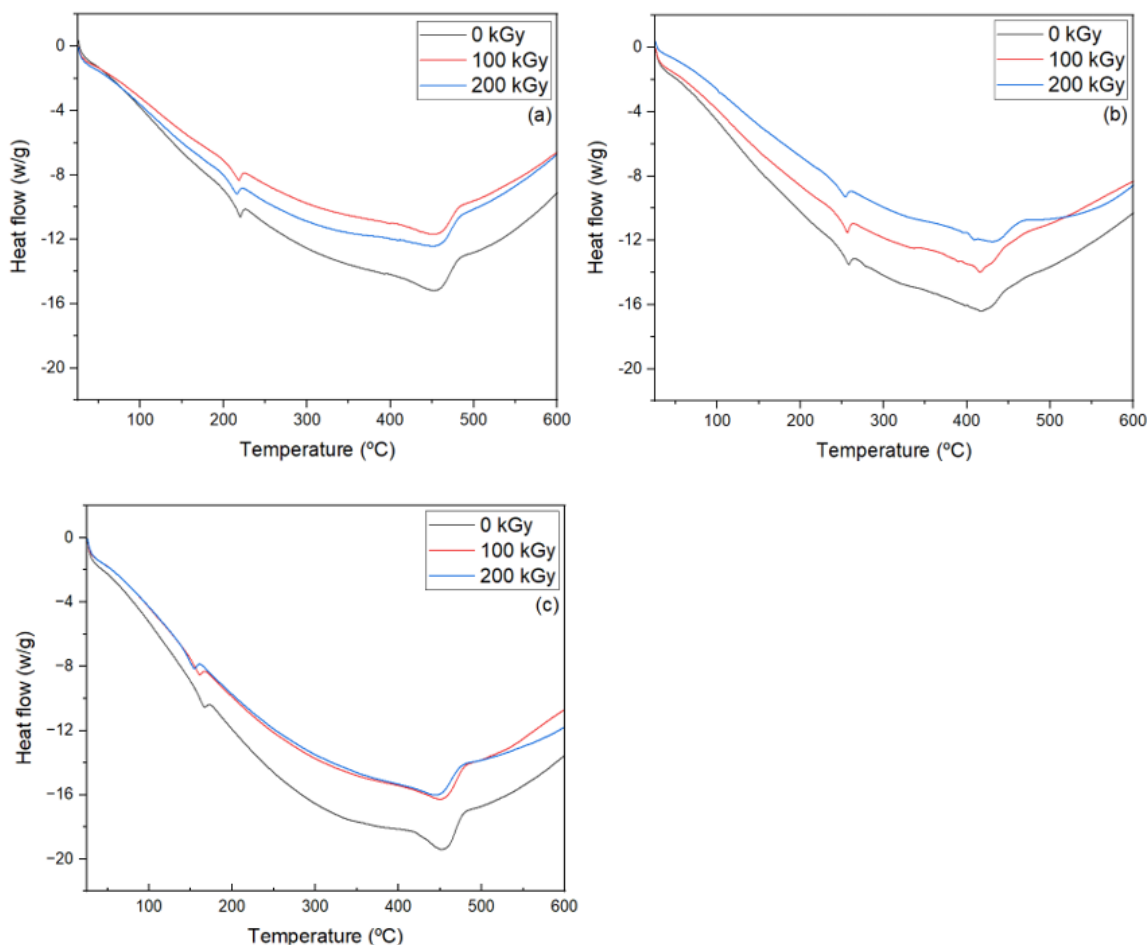



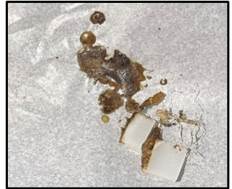




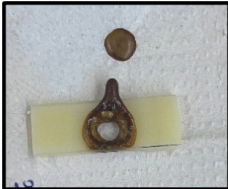

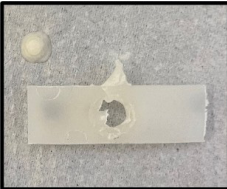






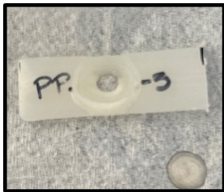

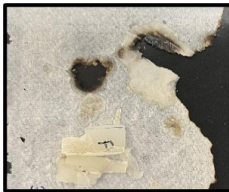
Figure 9. DSC curves of non-irradiated and irradiated PA-6 (a), PA-6.6 (b), and PP (c).

Table 2. Specimens after glow-wire testing at temperatures of 650, 750 and 850°C; a) 0 kGy, b) 100 kGy, c) 200 kGy for PA-6, PA-6.6 and PP samples.

Dose	Temp.	PA-6	PA-6.6	PP
	650°C			
		Approved	Approved	Approved
0 kGy	750°C			No image
		Failed	Approved	Failed ²
	850°C			No image
		Failed	Approved	Failed ²
	650°C			No image
		Failed	Approved	Approved ⁴
100 kGy	750°C	No image		
		Failed ¹	Failed	Approved
	850°C	No image	No image	
		Failed ¹	Failed ²	Failed

¹ Eliminated from the test due to failure at a temperature of 650°C ² Eliminated from the test due to failure at a temperature of 750°C ³ Test at 650°C not performed due to approval at temperatures of 750°C and 850°C ⁴ Test at 650°C not performed due to approval at a temperature of 750°C.

Table 2. Continued...

Dose	Temp.	PA-6	PA-6.6	PP
	650°C		No image	No image
		Approved	Approved ³	Approved ⁴
200 kGy	750°C			
		Failed	Approved	Approved
	850°C	No image		
		Failed ²	Approved	Failed

¹ Eliminated from the test due to failure at a temperature of 650°C ² Eliminated from the test due to failure at a temperature of 750°C ³ Test at 650°C not performed due to approval at temperatures of 750°C and 850°C ⁴ Test at 650°C not performed due to approval at a temperature of 750°C.

that the non-irradiated PA-6 sample was accepted only after the test at a temperature of 650°C. When the samples were irradiated at 100 kGy, the PA-6 behaved unsatisfactorily, failing at all three temperatures used in this test, 650, 750 and 850°C. When the PA-6 samples were irradiated at 200 kGy, the characteristics of the PA-6 sample remained similar to those of the non-irradiated samples, whose specimens passing only at a temperature of 650°C.

The non-irradiated PA-6.6 sample passed the test after being exposed to temperatures of 650 and 750°C and failed at 850°C. The sample irradiated with a dose of 100 kGy did not perform satisfactorily, because it passed only when the minimum temperature was 650°C, showing a lower performance than the non-irradiated sample. Fortunately, when the polyamide samples were subjected to a dose of 200 kGy, the PA-6.6 performed satisfactorily at all three temperatures studied (650, 750 and 850°C), being the single irradiated sample that achieved this level of performance (Table 2). According to the achieved analyses, the non-irradiated polypropylene passed only when it was subjected to a temperature of 650°C. The polypropylene samples irradiated at 100 and 200 kGy were approved in the tests carried out at temperatures of 650 and 750°C, which indicates improved performance.

3.5. Scratch test and profilometer analysis

The values of average apparent scratch coefficient of friction (SCOF) and the standard deviation for the permanent regime region (1 mm to 3 mm) were listed in Figures 10a-c, for the non-irradiated as well as for the EB irradiated 100 and 200 kGy samples of PA-6, PA-6.6, and PP. The results of SCOF values are shown in Table 3.

The SCOF results demonstrate that PA-6 (Figure 10a), after the irradiation at 100 and 200 kGy, shows a reduction in the average SCOF of 12.55 and 3.46%, respectively, compared to the non-irradiated samples. PA-6.6 irradiated with an irradiation dose of 100 kGy shows a reduction of 5.6% in the coefficient of friction. However, when the sample of PA-6.6 is irradiated at 200 kGy, there was found an increase of 18.69% in the value of this parameter is found. Figure 10b shows the SCOF curves for the PA-6.6 specimens. The PP samples, on the other hand, show an increase of 11.32 and 1.89% in the SCOF when they are irradiated at 100 and 200 kGy, respectively. Figure 10c presents the graph of the SCOF curves for the PP specimens. Motamedi and Bagheri³¹ studied the scratch deformation in pure PA-6 and PP blends, based on the stick-slip peaks mechanism. They identify the deformation mechanisms as a key factor in the influence of the scratch, impacted by various bulk mechanical properties.

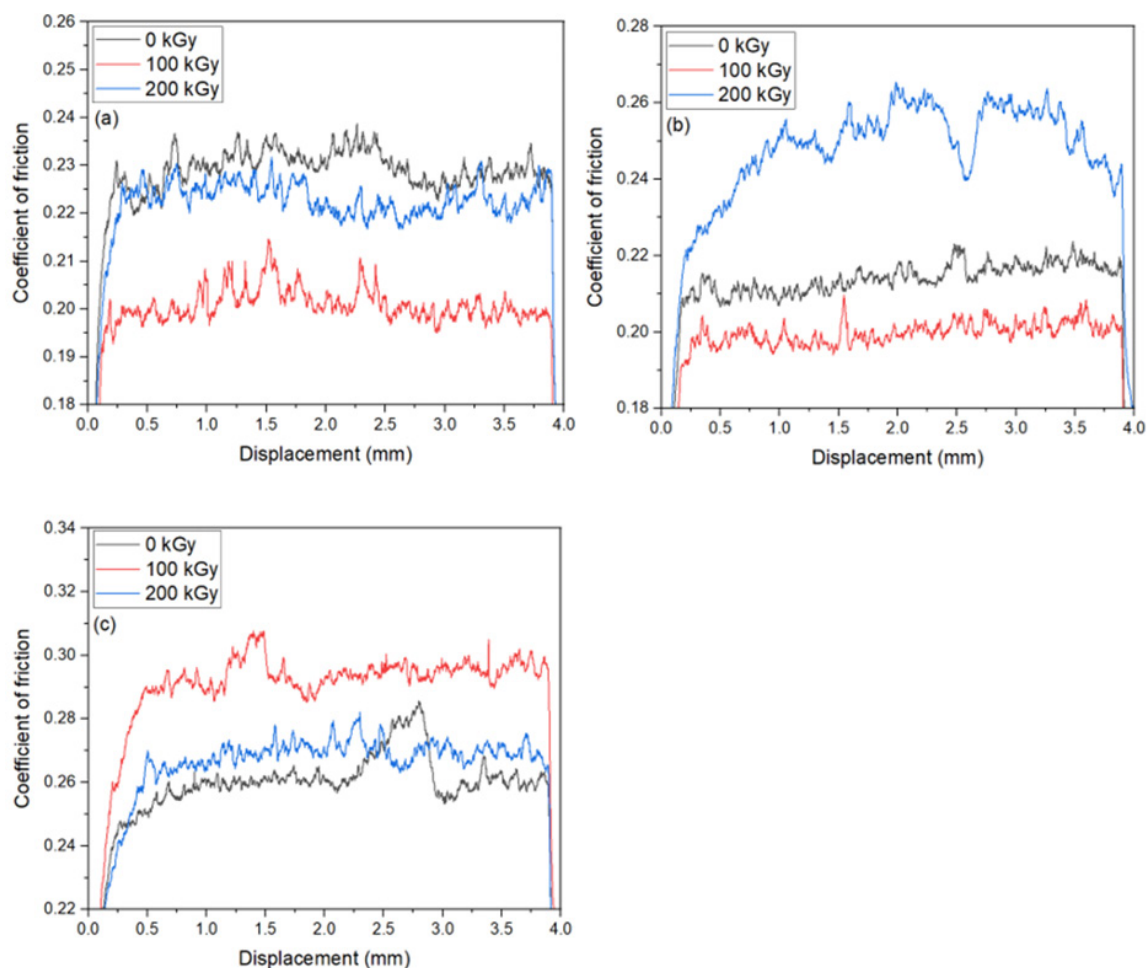


Figure 10. Coefficient of friction of non-irradiated and irradiated PA-6 (a), PA-6.6 (b), and PP (c).

Table 3. SCOF values for non-irradiated and 100 kGy and 200 kGy irradiated samples of PA-6, PA-6.6, and PP.

Dose (kGy)	SCOF values		
	PA-6	PA-6.6	PP
0	0.231 ± 0.003	0.214 ± 0.003	0.265 ± 0.008
100	0.202 ± 0.004	0.200 ± 0.003	0.295 ± 0.005
200	0.223 ± 0.003	0.254 ± 0.006	0.270 ± 0.003

The scratch resistance of polymers depends on constitutive injection molding and surface properties, such as the SCOF values^{14,32}. Dasari et al.¹⁸ carried out a comparative assessment of scratch damage, taking into consideration the average surface height of the damaged region, the depth, and thickness of the tracks. They also consider that high-crystallinity polypropylene is more mechanically resistant to the induced surface damage than low-crystallinity polypropylene. However, the experimental results from the irradiated polypropylene samples did not align with the findings reported by Dasari et al.¹⁸. It was found that the percentage of crystallinity increased after irradiation at applied doses of 100 and 200 kGy. However, the changes in scratch width were very small (centesimal variation of 0.01), and scratch depth was reduced only when the material

was irradiated with 200 kGy. Khatri and Sue³² demonstrated that the scratch groove involves depth and shoulder height, dependent on polymer mechanical properties, surface, and polymer flow characteristics in the injection molding process. The scratch hardness provides only partial understanding. It fails to account for the critical recovery properties displayed by various polymeric materials¹⁴, where the smooth curves indicate the plastic deformation of the polymers without notable failure¹⁵. In this case, the surface roughness is directly dependent on scratch visibility and opposite to the gloss level of the surface¹⁸.

For the textured samples, a 3D-scratch test was performed, showing depth and dimensions due to the non-uniform surface topology (Figure 11). Guru and Sarangi¹⁵ show the importance of the smooth curves that reflect the plastic deformation of

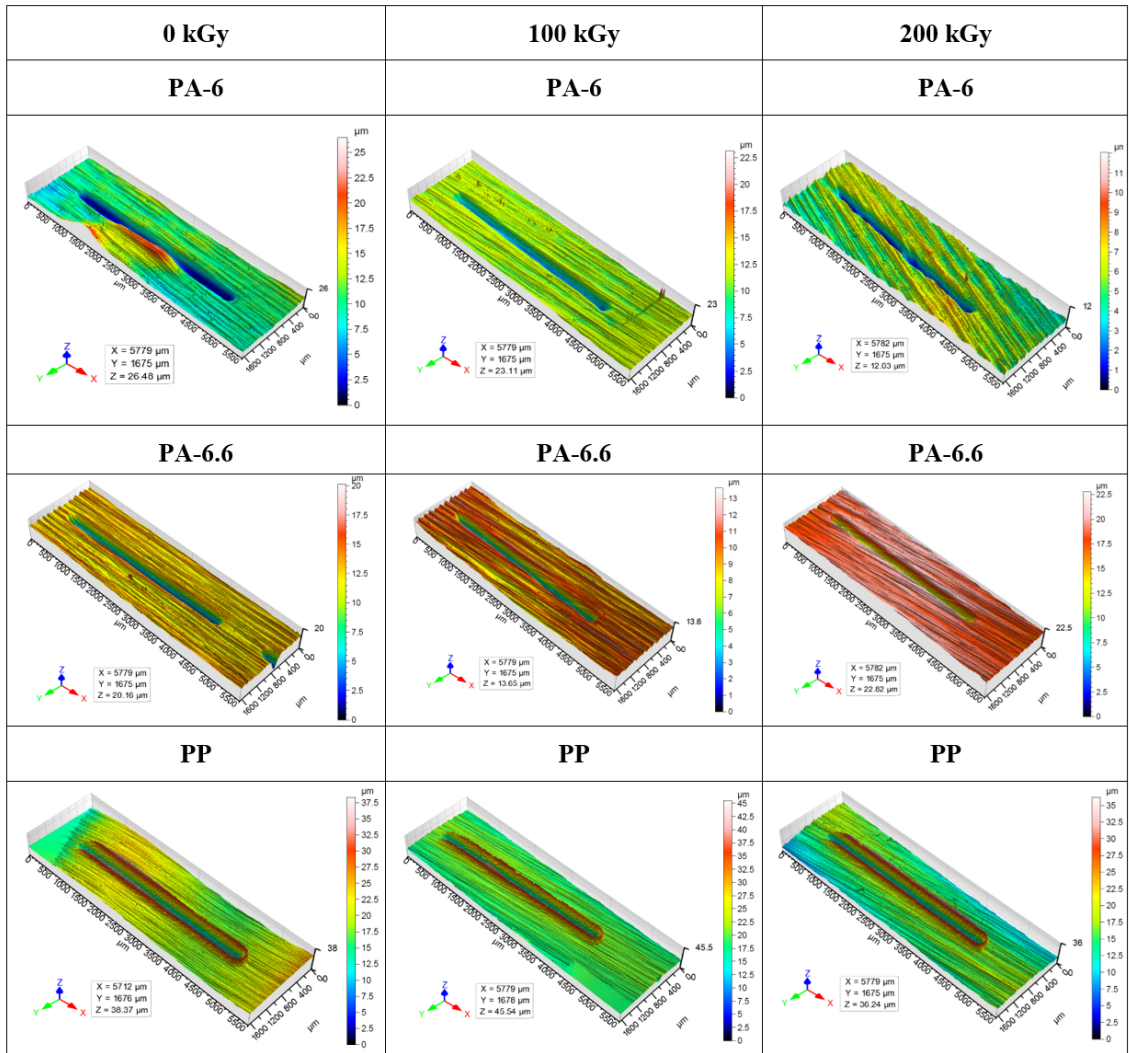


Figure 11. 3D-SCOF view of surface friction of non-irradiated and irradiated PA-6, PA-6.6, and PP.

Table 4. Width and depth SCOF-values for non-irradiated and 100 and 200 kGy irradiated specimens of PA-6, PA-6.6, and PP.

Specimen	Dose (kGy)	Width (mm)	Depth (µm)
PA-6	0	4.28	9.42
	100	4.33	7.65
	200	4.20	5.38
PA-6.6	0	4.27	1.34
	100	4.25	0.93
	200	4.24	1.80
PP	0	4.18	2.70
	100	4.19	3.32
	200	4.17	1.91

the polymers without any significant failure, while all these variables show a linear increase as the load rises.

In this study, the 3D-SCOF parameter is utilized for data validation (Table 4), and digital images are captured to document the surface characteristics of each specimen. For the apparent 3D-scratch coefficient of friction (3D-SCOF)

view, PA-6 irradiated at 100 kGy shows an increase in the width of the scratch, while the depth was reduced. When irradiated with a dose of 200 kGy, there was a reduction of 1.87% in the width and 42.89% in the depth of the scratch.

PA-6.6 irradiated at a dose of 100 kGy shows a reduction of 0.47% in width and a 30.60% reduction in its scratch

depth. At a dose of 200 kGy, only the width of the scratch was reduced. The PP specimen irradiated with a dose of 100 kGy showed an increase in both scratch width and depth. At a dose of 200 kGy, there was a slight reduction in width and a 29.26% reduction in scratch depth. The PP samples show high plastic deformity, with high red stick-slip in the border-scratch test caused by modification induced by EB irradiation and plastic deformation in all samples¹⁶. Jiang et al.¹⁶ described that the accumulated material in front of the tip hinders its horizontal movement and adds an extra resistance force. To enable the scratch tip to move forward again, the friction and resistance from the material must be overcome. Gao et al.¹⁷ investigated that a periodic fish-scale pattern caused by stick-slip always occurs in scratching PP-based materials. Otherwise, some polymer scraps were formed under high forces, -or the stress-whitening is minimal when the load applied to the PP is 10 N or less.

4. Conclusion

FTIR spectroscopy showed a slight degradation of the PP samples, in the 2700-3000 cm^{-1} range; and chemical stability was indicated by the presence of carbonyl groups in vibration belt 1736 cm^{-1} , for PA-6 and PA-6.6 samples, after the irradiation process. The chain scission and crosslinking took place simultaneously during irradiation, when chain scission being predominant below T_{onset} . The chain crosslinking at 100 and 200 kGy showed a significant decrease with rising as the absorbed dose is growing up, based on the investigated thermal properties. The mechanical properties of the PP samples, for example, the tensile tests, could not be carried out because the irradiated samples became brittle and broke when they were placed in the test equipment. There was a decrease in the material properties related to flexural strength, degradation temperature, and melting temperature for PA-6 and PA-6.6. Only flexural strength showed an increase for PA-6 specimens. The results only indicated an increase in the percentage of crystallinity and resistance to glow wire for all samples evaluated with a 200 kGy irradiation dose. The results for all samples also showed a slight reduction in the average SCOF width, scratch depth, and width with the 100 kGy dose; however, with the 200 kGy dose, there was an increase in the average friction coefficient and scratch depth.

Finally, it was concluded that among the three materials studied, PA-6.6 showed the best performance after EB irradiation, excelling in the physical and thermal tests. On the other hand, PA-6 and PP samples did not show significant results after the irradiation process.

5. Acknowledgments

The authors would like to thank Thermoblend®, Henkel®, and LFS-EPUSP. We also thank CAPES and CNEN for their financial support.

6. References

- Burillo G, Adem E, Muñoz E, Vásquez M. Electron beam irradiated polyamide-6 at different temperatures. *Radiat Phys Chem.* 2013;84:140-4. <http://doi.org/10.1016/j.radphyschem.2012.06.029>.
- Pramanik N, Haldar R, Bhardwaj Y, Sabharwal S, Niyogi U, Khandal R. Radiation processing of Nylon 6 by e-beam for improved properties and performance. *Radiat Phys Chem.* 2009;78(3):199-205. <http://doi.org/10.1016/j.radphyschem.2008.11.004>.
- Bednarik M, Pata V, Ovsik M, Mizera A, Husar J, Manas M, et al. The modification of useful injection-molded parts' properties induced using high-energy radiation. *Polymers.* 2024;16(4):450. <http://doi.org/10.3390/polym16040450>.
- Adem E, Burillo G, del Castillo L, Vásquez M, Avalos-Borja M, Marcos-Fernández A. Polyamide-6: the effects on mechanical and physicochemical properties by electron beam irradiation at different temperatures. *Radiat Phys Chem.* 2014;97:165-71. <http://doi.org/10.1016/j.radphyschem.2013.11.008>.
- Kumar R. Nano scale free volume study of high energy (MeV) ion beam irradiated polyamide nylon-6 polymer. *Indian J Pure Appl Phys.* 2010;48(4):233-9.
- Ovsik M, Stanek M, Bednarik M. Evaluation of cross-linked polyamide 6 micro-indentation properties: TAIC concentration and electron radiation intensity. *Materials.* 2023;16(6):2391. <http://doi.org/10.3390/ma16062391>.
- Santos AF. Efeito da irradiação por feixe de elétrons sobre as propriedades físicas e químicas de uma resina de polipropileno [dissertation]. São Paulo: Universidade de São Paulo; 2011.
- Svoboda P, Trivedi K, Stoklasa K, Svobodova D, Ougizawa T. Study of crystallization behaviour of electron beam irradiated polypropylene and high-density polyethylene. *R Soc Open Sci.* 2021;8(3):202250. <http://doi.org/10.1098/rsos.202250>.
- Elhady M, Elbarbary A, Gad Y, Fathy E. Synthesis and impact of polyethylene terephthalate nanoparticles on the stability of polypropylene exposed to electron beam irradiation. *Polym Degrad Stabil.* 2022;202:110012. <http://doi.org/10.1016/j.polymdegradstab.2022.110012>.
- Pramanik N, Haldar R, Niyogi U, Alam M. Development of an advanced engineering polymer from the modification of nylon 66 by e-beam irradiation. *Def Sci J.* 2014;64(3):281-9. <http://doi.org/10.14429/dsj.64.7328>.
- Zaharescu T, Silva L, Jipa S, Kappel W. Post-irradiation thermal degradation of PA6 and PA6.6. *Radiat Phys Chem.* 2010;79(3):388-91. <http://doi.org/10.1016/j.radphyschem.2009.08.041>.
- Porubská M, Szöllos O, Kónová A, Janigová I, Jašková M, Jomová K, et al. FTIR spectroscopy study of polyamide-6 irradiated by electron and proton beams. *Polym Degrad Stabil.* 2012;97(4):523-31. <http://doi.org/10.1016/j.polymdegradstab.2012.01.017>.
- Bradler P, Fischer J, Wallner G, Lang R. Effect of irradiation induced cross-linking on the properties of different polyamide grades. *Mater Today Proc.* 2019;10:441-7. <http://doi.org/10.1016/j.matpr.2019.03.008>.
- Andena L, Chiarot G. Scratch hardness as a quasi-intrinsic parameter to measure the scratch resistance of polymers. *Wear.* 2023;514-515:204562. <http://doi.org/10.1016/j.wear.2022.204562>.
- Guru S, Sarangi M. Evaluation of hardness and elastic modulus of polymer materials through micro-scratch method: an empirical study. *Polymer-Plast Technol Mater.* 2024;64(4):574-91. <http://doi.org/10.1080/25740881.2024.2420788>.
- Jiang H, Cheng Q, Jiang C, Zhang J, Yonghua L. Effect of stick-slip on the scratch performance of polypropylene. *Tribol Int.* 2015;91:1-5. <http://doi.org/10.1016/j.triboint.2015.06.024>.
- Gao W, Wang L, Coffey J, Daver F. Finite element simulation of scratch on polypropylene panels. *Mater Des.* 2018;140:400-8. <http://doi.org/10.1016/j.matdes.2017.12.018>.
- Dasari A, Rohmann J, Misra R. Micro- and nanoscale evaluation of scratch damage in poly(propylene)s. *Macromol Mater Eng.* 2002;287(12):889-903. <http://doi.org/10.1002/mame.200290024>.
- Sirin M, Zeybek M, Sirin K, Abali Y. Effect of gamma irradiation on the thermal and mechanical behaviour of polypropylene and polyethylene blends. *Radiat Phys Chem.* 2022;194:110034. <http://doi.org/10.1016/j.radphyschem.2022.110034>.
- Araújo MS, Ferro WP, Wiebeck H, Zen HA, Pioltini G. Pequeno manual do náilon: São Paulo: Editora Artliber; 2021.

21. Socrates G. Infrared and Raman characteristic group frequencies: tables and charts. Chichester: Wiley; 2001.
22. Pavia DL, Lampman GM, Kriz GS, Vyvyan JR. Introdução à espectroscopia. 4. ed. São Paulo: Cengage Learning; 2010.
23. Albano C, Perera R, Silva P, Sánchez Y. Characterization of irradiated PEs/PA6 blends. *Polym Bull.* 2006;57(6):901-12. <http://doi.org/10.1007/s00289-006-0651-y>.
24. Porubská M, Szöllös O, Janigová I, Jomová K, Chodák I. Crosslinking of polyamide-6 initiated by proton beam irradiation. *Radiat Phys Chem.* 2017;133:52-7. <http://doi.org/10.1016/j.radphyschem.2016.12.010>.
25. Massoud A, Maziad N, Othman M, Borai E. Estimation of gamma radiation effects on the polypropylene (PP) films at various doses. *J Macromol Sci Part A Pure Appl Chem.* 2024;61(12):1005-18. <http://doi.org/10.1080/10601325.2024.2419531>.
26. Pino ES, Colombo SMA. Mechanical properties of electron beam irradiated Polyamide 6,6. Vienna: International Atomic Energy Agency; 2006.
27. Sengupta R, Sabharwal S, Tikku V, Somani A, Chaki T, Bhowmick A. Effect of ambient-temperature and high-temperature electron-beam radiation on the structural, thermal, mechanical, and dynamic mechanical properties of injection-molded polyamide-6,6. *J Appl Polym Sci.* 2006;99(4):1633-44. <http://doi.org/10.1002/app.22689>.
28. Ferro WP. Utilização da cinza da casca de arroz como carga em matriz de poliamida 6 submetida à radiação ionizante [dissertation]. São Paulo: Universidade de São Paulo; 2009.
29. Park EH, Kim SB, Choi Y-T, Park E-S. Effects of electron beam irradiation on thermal and mechanical properties of nylon 6, nylon 66 and nylon 1212. *Res Rev Polymer.* 2016;7(1):7-19.
30. Lugão A, Hutzler B, Ojeda T, Tokumoto S, Siemens R, Makuuchi K, et al. Reaction mechanism and rheological properties of polypropylene irradiated under various atmospheres. *Radiat Phys Chem.* 2000;57(3-6):389-92. [http://doi.org/10.1016/S0969-806X\(99\)00473-9](http://doi.org/10.1016/S0969-806X(99)00473-9).
31. Motamedi P, Bagheri R. Study of the scratch resistance criteria and their relationship with mechanical properties and microstructure in a ternary thermoplastic blend. *Wear.* 2017;386-387:118-28. <http://doi.org/10.1016/j.wear.2017.06.008>.
32. Khatri S, Sue H. Scratch visibility modeling on flat & textured polymeric surfaces. *Polymer.* 2024;312:127595. <http://doi.org/10.1016/j.polymer.2024.127595>.

Data Availability

The complete dataset supporting the findings of this study has been published in the article and in the “Supplementary Materials” section.

Supplementary material

The following online material is available for this article:

Table S1 - Statistical data of the PA-6 for tensile stress at break, stretching and stress at the point yield.

Table S2 - Statistical data of the PA-6.6 for tensile stress at break, stretching and stress at the point yield.

Table S3 - Statistical data of flexure stress of PA-6, PA-6.6 and PP.

Table S4 - TGA data (°C) for initial T_{onset} and final T_{endset} .

Table S5 - Crystallinity (%) and melting point by DSC analysis for the non-irradiated, 100 kGy, and 200 kGy irradiated samples of PA-6, PA-6.6, and PP.